

Ultrafast electron diffraction of photoexcited gas-phase cyclobutanone predicted by *ab initio* multiple cloning simulations

Dmitry V. Makhov,^{1,2} Adam Kirrander,³ and Dmitrii V. Shalashilin¹

¹*School of Chemistry, University of Leeds, Leeds LS2 9JT, United Kingdom*

²*School of Mathematics, University of Bristol, Fry Building, Woodland Road, Bristol, BS8 1UG, United Kingdom*

³*Physical and Theoretical Chemistry Laboratory, Department of Chemistry, University of Oxford, Oxford OX1 3QZ, United Kingdom.*

(*Electronic mail: d.makhov@leeds.ac.uk)

(Dated: 19 February 2024)

We present the result of our calculations of ultrafast electron diffraction (UED) for cyclobutanone excited into S_2 electronic state, which are based on the non-adiabatic dynamics simulations with *Ab Initio* Multiple Cloning (AIMC) method with the electronic structure calculated at the SA(3)-CASSCF(12,12)/aug-cc-pVDZ level of theory. The key features in the UED pattern were identified that can be used to distinguish between the reaction pathways observed in the AIMC dynamics, although there is a significant overlap between representative signals due to structural similarity of the products. The calculated UED pattern can be compared with experiment.

I. INTRODUCTION

Ultrafast electron diffraction (UED) has evolved into a powerful method for structural dynamics.^{1,2} Although UED, and the closely related method of ultrafast x-ray scattering,^{3,4} arguably provide the most direct access to structural dynamics in photoexcited molecules, the interpretation of experiments is nontrivial. Despite significant progress in the development of inverse methods, which aim to produce a (time-dependent) molecular model commensurate with the experimental data,⁵⁻⁹ the gold standard for interpreting ultrafast experiments remains comparison to high-quality simulations of the photoexcited target molecule. However, such simulations remain challenging, and their veracity depends keenly on numerous methodological choices. As a much needed step towards surveying and evaluating good practice, the Journal of Chemical Physics recently announced the *Prediction Challenge: Cyclobutanone Photochemistry* to which this paper is a response.

The challenge is motivated by an experiment at the SLAC Megaelectronvolt ultrafast electron diffraction (SLAC MeV-UED) facility, where a gas-phase sample of cyclobutanone is irradiated with a 200 nm laser pulse and a time-resolved UED signals are recorded. At this excitation energy, a low-lying $n \rightarrow 3s$ (S_2) Rydberg state in cyclobutanone is excited.¹⁰⁻¹³ The photochemistry of cyclobutanone has a long history, with early experiments carried out in the 1940s,¹⁴ with particular attention having been paid to the photoproducts of the reaction.¹⁴⁻¹⁹

In this work, the photodynamics of cyclobutanone is simulated using *Ab initio* Multiple cloning (AIMC)²⁰⁻²² approach, which is in principle a fully quantum, formally exact methodology based on using Gaussian Coherent States propagated by Ehrenfest trajectories as a basis for quantum dynamics of nuclear wave functions. AIMC was successfully applied before²³⁻²⁷ to simulate the process of the photodissociation of a number of heterocyclic molecules. Based on AIMC dynamics results, the gas phase time-resolved UED pattern of cyclobutanone photoexcited using a 200 nm pulse is calculated for the initial 200 fs of dynamics, allowing for direct

comparison to experimental data.

II. THEORETICAL METHODS

A. AIMC

As the AIMC methodology was extensively described before²⁰⁻²³, here we provide only a summary of the technique. The AIMC method represents the further development of the Multi Configurational Ehrenfest (MCE)²⁸⁻³¹ approach and makes use of the following wave-function ansatz:

$$|\Psi(\mathbf{R}, \mathbf{r}, t)\rangle = \sum_n c_n(t) |\chi(\mathbf{R}, t)\rangle \sum_I a_I^{(n)} |\phi_I(\mathbf{r}; \mathbf{R})\rangle, \quad (1)$$

where \mathbf{R} and \mathbf{r} are electronic and nuclear coordinates respectively. The electronic part of each basis function is represented in a basis of adiabatic electronic states $|\phi_I\rangle$, and the nuclear parts is a moving Gaussian Coherent State:

$$|\chi_n(\mathbf{R}, t)\rangle = \left(\frac{2\alpha}{\pi}\right)^{\frac{N_{\text{dof}}}{4}} \times \exp\left(-\alpha(\mathbf{R} - \mathbf{R}_n)^2 + \frac{i}{\hbar} \mathbf{P}_n(\mathbf{R} - \mathbf{R}_n) + \frac{i}{\hbar} \gamma_n(t)\right), \quad (2)$$

which is a Gaussian-shaped de Broglie wave centred at \mathbf{R}_n with momentum \mathbf{P}_n and phase γ_n . The motion of Gaussians $|\chi_n\rangle$ is guided by the Ehrenfest force:

$$\dot{\mathbf{R}}_n = M^{(-1)} \mathbf{P}_n,$$

$$\dot{\mathbf{P}}_n = - \sum_I |a_I^{(n)}|^2 \nabla V_I^{(n)} + \sum_{I \neq J} a_I^{(n)*} a_J^{(n)} \mathbf{d}_{IJ}^{(n)} \cdot \dot{\mathbf{R}}_n \left(V_I^{(n)} - V_J^{(n)} \right), \quad (3)$$

where V_I is potential energy surface of the I th electronic state, \mathbf{d}_{IJ} a non-adiabatic coupling vector, and M is a diagonal matrix of atomic masses. As the force depends on Ehrenfest amplitudes $a_I^{(n)}$, the equations of motion (3) must be solved simultaneously with the equations for $a_I^{(n)}$:

$$\dot{a}_I^{(n)} = -\frac{i}{\hbar} V_I^{(n)} a_I^{(n)} - \sum_J \dot{\mathbf{R}}_n \cdot \mathbf{d}_{IJ} a_J^{(n)}, \quad (4)$$

where the right side is the electronic Hamiltonian for n th basis function. Finally, phase γ_n is propagated semiclassically as $\dot{\gamma}_n = \mathbf{P}_n \dot{\mathbf{R}}_n / 2$.

It is well known that Ehrenfest trajectories misguide basis set when several non-interacting electronic states have significant amplitudes. The cloning procedure is applied in AIMC approach in order to address this issue. In principle, the cloning can be viewed as straightforward way of spawning employed in the Multiple Spawning method³². The idea of cloning is to replace a basis function with two clones, each of which is guided in most by just one potential energy surface. In the simplest case of two electronic states:

$$\begin{aligned} c_n |\chi_n\rangle \left(a_1^{(n)} |\phi_1\rangle + a_2^{(n)} |\phi_2\rangle \right) = \\ c'_n |\chi_n\rangle \left(0 \times |\phi_1\rangle + \frac{a_2^{(n)}}{|a_2^{(n)}|} |\phi_2\rangle \right) \\ + c''_n |\chi_n\rangle \left(\frac{a_1^{(n)}}{|a_1^{(n)}|} |\phi_1\rangle + 0 \times |\phi_2\rangle \right), \end{aligned} \quad (5)$$

where

$$c'_n = c_n |a_2^{(n)}|; c''_n = c_n |a_1^{(n)}|. \quad (6)$$

The total contribution of two clones into wave function $|\Psi(\mathbf{R}, \mathbf{r}, t)\rangle$ is exactly the same as that of the original basis function. However, cloning increases the size of basis set creating additional flexibility, as two clones can now move in different directions. The cloning is applied when the breaking force $\mathbf{F}_I^{(br)} = |a_I|^2 (\nabla V_I - \sum_J |a_J|^2 \nabla V_J)$ exceeds a threshold and, at the same time, the magnitude of non-adiabatic coupling is below a second threshold. Cloning is an extremely important part of AIMC method, as it allows AIMC to reproduce the bifurcation of the wave function at conical intersections.

The trajectories in AIMC approach can be calculated independently using potential energies forces and non-adiabatic coupling vectors calculated ‘‘on the fly’’ by an electronic structure code. Then, time-dependent Schrödinger equation for amplitudes c_n is solved in post-processing in the precalculated trajectory-guided basis (1).

In practice to achieve good convergence, a number of sampling techniques have to be used. Swarms of coupled trajectory guided Gaussians, as well as their train guided by the same trajectories are among those techniques³³. It has been demonstrated that MCE can produced the results, which are well converged³⁴ and AIMC, its *ab initio* direct dynamics version, is more accurate than Surface Hopping or Ehrenfest Dynamics^{35,36}. A technique which allows to take into

account pulse shape and dynamics which occur during the excitation has been developed³⁷. In its simplest form, which is used in the present paper, AIMC can yield qualitative or semi-quantitative picture of the process, similar to that given by Surface Hopping, *Ab initio* Multiple Spawning (AIMS)³² and many other popular techniques.

B. Ultrafast electron diffraction

For the modelling of the UED signals, we anticipate that the experimental data in this challenge can be modelled reliably using the independent atom model (IAM). This approximates the scattering signal as a coherent sum of scattering from isolated atoms centered at the positions of the nuclei in the target molecule. Notably, this model excludes the contribution of the bonding electrons and the characteristics of the electronic states of the molecule. Should the quality of the experimental data necessitate that these effects are accounted for, then numerical codes capable of this exist,^{38–41} albeit at significantly higher computational cost.

The total (energy-integrated) scattering cross section into the solid angle $d\Omega$ at time t is given by,^{42–44}

$$\frac{d\sigma}{d\Omega} \bigg/ \left(\frac{d\sigma}{d\Omega} \right)_{\text{Rh}} = I_{\text{tot}}(\mathbf{s}, t), \quad (7)$$

where $\mathbf{s} = \mathbf{k}_0 - \mathbf{k}_1$ is the scattering vector expressed in terms of the wave vectors of the incoming and outgoing electrons. The scattering is given in units of the Rutherford cross section $(d\sigma/d\Omega)_{\text{Rh}}$ which includes the s^{-4} scaling factor.^{45,46} Note that the expression above does not account for the duration of the electron pulse, which may be accounted for via a temporal convolution of the predicted signal by the instrument response function for the experiment.

General expressions that account for the full wavefunction in Eq. (1), including the non-local nature of the individual Gaussian coherent states, have been derived previously.⁴² Given the sparse basis used in the present simulations, we resort here to the diagonal bracket-averaged Taylor (BAT) expansion approximation⁴² and assume that expansion coefficients are independent of time, $c_n \approx c_n(t)$, giving the total scattering intensity as,

$$I_{\text{tot}}(\mathbf{s}, t) = \sum_{n=1} |c_n|^2 I_n(\mathbf{s}, \mathbf{R}_n(t)). \quad (8)$$

In this simplified form, sufficient for our present needs, the scattering from each trajectory is given by IAM as,⁴⁷

$$I_n(\mathbf{s}, \mathbf{R}_n(t)) = |F(\mathbf{s}, \mathbf{R}_n(t))|^2 + S_{\text{inel}}(s), \quad (9)$$

where $S_{\text{inel}}(s)$ is the inelastic scattering, which is independent of molecular geometry and isotropic, as underscored by its dependence only on the amplitude of the momentum transfer vector, $s = |\mathbf{s}|$. It is given by an incoherent summation over the individual atomic contributions,

$$S_{\text{inel}}(s) = \sum_{A=1}^{N_{\text{at}}} S_A(s), \quad (10)$$

with N_{at} the number of atoms in the molecule. The corresponding elastic contribution is given by the form factor $F(\mathbf{s}, \mathbf{R}_n(t))$,

$$F(\mathbf{s}, \mathbf{R}_n(t)) = \sum_{A=1}^{N_{\text{at}}} f_A^e(s) e^{i\mathbf{s}\mathbf{R}_{nA}(t)}, \quad (11)$$

where $f_A^e(s)$ are the atomic form factors and $\mathbf{R}_{nA}(t)$ the position vector for atom A in trajectory n . The form factors for electron scattering are $f_A^e = (f_A^x - Z_A)$, where f_A^x the x-ray scattering form factor and Z_A is the atomic number.^{45,46} Both $f_A^x(s)$ and $S_A(s)$ are tabulated.⁴⁸ For high energy electron scattering it is sometimes necessary to use form factors with relativistic corrections,^{49,50} but this is not done presently.

When the target is a gas of anisotropic molecules, $|F(\mathbf{s}, \mathbf{R}_n(t))|^2$ in Eq. (9) is replaced by its rotationally averaged counterpart, $\langle |F(s, \mathbf{R}_n(t))|^2 \rangle$,⁵¹

$$\langle |F(s, \mathbf{R}_n(t))|^2 \rangle = \sum_{A,B} f_A^e(s) f_B^e(s) \frac{\sin(sR_{nAB}(t))}{sR_{nAB}(t)} \quad (12)$$

where $R_{nAB}(t) = |\mathbf{R}_{nA}(t) - \mathbf{R}_{nB}(t)|$ is the distance between atoms A and B in trajectory n .

III. COMPUTATIONAL DETAILS

The trajectories were calculated using our own AIMC code, where potential energies, forces and non-adiabatic couplings given “on the fly” by MOLPRO⁵² electronic structure package at SA(3)-CASSCF(12,12)/aug-cc-pVDZ level of theory. We note that the electronic structure method has been benchmarked in another paper submitted to the same challenge by one of the co-authors (AK). In brief, three electronic states were taken into consideration, a ground state and two lowest singlet excited states. Higher energy Rydberg states have been shown to exist (3p character) but have been shown to be unimportant for dynamics after excitation into S_2 , therefore we do not include them in our simulations.⁵³ We also do not take triplet states into consideration in this work, as they have been shown to only play a role in dynamics upon excitation with long wavelengths.¹⁹ The initial positions and momenta for all trajectories are randomly sampled from the ground state vibrational Wigner distribution using vibrational frequencies and normal modes calculated at the same level of theory. This ground state wavepacket is then simply lifted to the second excited state within Condon approximation. As in our previous simulations^{20,23–27} the cloning thresholds were taken as $5 \cdot 10^{-6}$ a.u. and $2 \cdot 10^{-3}$ a.u. for the magnitude of breaking force and non-adiabatic coupling, respectively.

In *ab initio* dynamics, the number of trajectories is severely limited by the high cost of electronic structure calculations (especially for larger molecules). When the initial multi-dimensional wave-function is randomly sampled with a small number of Gaussians, these Gaussians will be located far away from each other with no coupling between them. Running Gaussians closer together would be an inefficient use of CPU time unless we need to reproduce a particular quantum effect

of the nuclear motion. In this work, we use a simplified semiclassical version of AIMC, where we do not consider the coupling between the trajectories. Instead, each branch simply gets its amplitudes at the time of cloning, and this amplitude determines the statistical weight of that brunch.

We initially run an ensemble of 39 Efronfest trajectories, which give rise to 121 branches in the process of cloning. All trajectories were propagated for 200 fs with 0.06 fs (2.5 a.u.) timestep. A relatively small number of trajectories and short duration of the dynamics is due to the strict deadline for this work. Nevertheless, despite not very good statistics, our calculations show clear UED patterns for the cyclobutanone photodynamics.

IV. RESULTS AND DISCUSSION

A. Dynamics

Figure 1 presents the dynamics of the populations for S_0 , S_1 and S_2 electronic states. For the first 25 fs of dynamics, the molecules stay in S_2 state, then $S_2 \rightarrow S_1$ population transfer starts. The growing population of S_1 state immediately initiate the next step of population transfer, from S_1 into the ground state. Within next 10 fs, the S_1 state population reaches the equilibrium level of about 20%, when the rates of $S_2 \rightarrow S_1$ and $S_1 \rightarrow S_0$ transfers are about the same. For the rest of our dynamics, the S_1 state population is fluctuating around this level, while S_2 state exhibit the exponential decay into a ground state $S_2 \rightarrow S_1 \rightarrow S_0$.

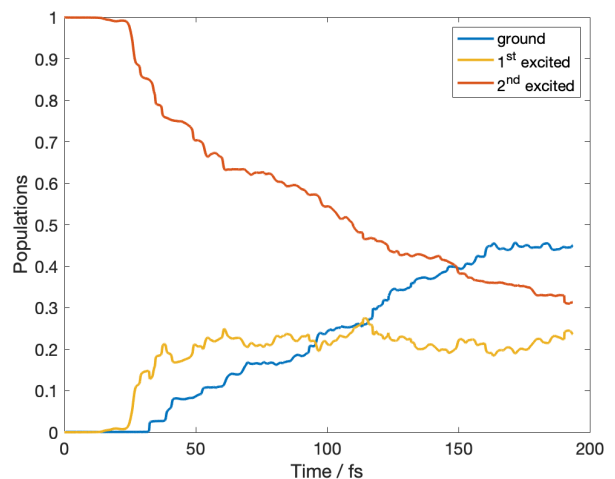


FIG. 1. The dynamics of S_2 (red), S_1 (yellow) and S_0 (blue) electronic state populations for cyclobutanone molecule after its photoexcitation into S_2 state.

Figure 2 shows the dynamics of C-C bonds breaking in the cyclobutanone ring. The bond is considered broken when the distance between two atoms exceeds 3 Å. The process of ring opening starts at about 25 fs time, simultaneously with the beginning of the non-adiabatic decay of S_2 state, by breaking β -CC bonds. Within next 50 fs, 30% of these bonds

break, which corresponds to 60% of the opened rings. At this stage of the dynamics, α -CC bonds are starting to break; this happens mostly in already opened rings creating ethylene (CH_2)(CH_2) and ethenone (CO)(CH_2) molecules. In some of these ethenone molecules, $\text{C}=\text{C}$ bonds also later break, creating CO and CH_2 radicals.

After about 100 fs time, some opened rings are beginning to close again (or, at least, their ends approach each other to less than 3 Å). Later, the ring can open again, creating an oscillatory behaviour in the number of broken bonds.

By the end of the dynamics, the yield in the (CH_2)(CH_2) + (CO)(CH_2) dissociation channel is 40.6%, the yield in the (CH_2)(CH_2) + (CO) + (CH_2) dissociation channel is 3.5%, and the yield of ring opening is 31.0%; also 17.2% molecules have remained in the closed ring form. The remaining 7.7% are found at various other intermediate configurations at the end of our 200 fs dynamics; the longer-term dynamics will be a subject of our future work.

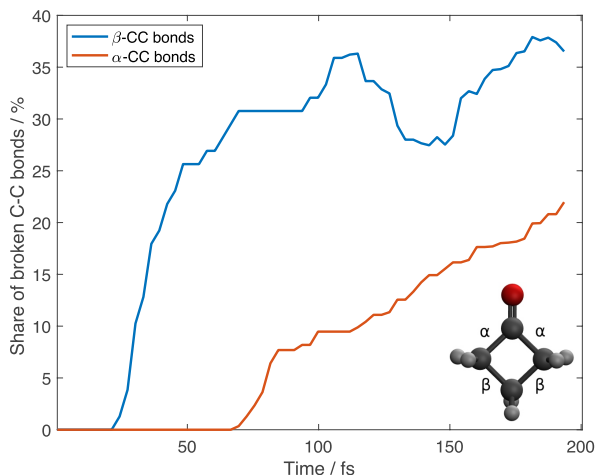


FIG. 2. The share of broken α - (red) and β - (blue) CC bonds as a function of time for cyclobutanone molecule after its photoexcitation into S_2 state.

B. Ultrafast electron diffraction

The AIMC simulations presented in section IV A serve as a framework to calculate the total rotationally averaged UED pattern for cyclobutanone, using the methodology presented in Section II B. The UED signal thus obtained is given in Fig. 3, plotted as percent difference $\%I_{\text{tot}}(s,t)$,

$$\%I_{\text{tot}}(s,t) = 100 \times \frac{I_{\text{tot}}(s,t) - I_{\text{tot}}(s,0)}{I_{\text{tot}}(s,0)}, \quad (13)$$

where, $I_{\text{tot}}(s,t)$ is the signal at time t and $I_{\text{tot}}(s,0)$ is the reference signal at $t = 0$, i.e. the pump-off signal.

To aid the interpretation of Fig. 3, we have also calculated the static signal for all reaction products observed in the AIMC simulations, shown in Fig. 4. Representative structures

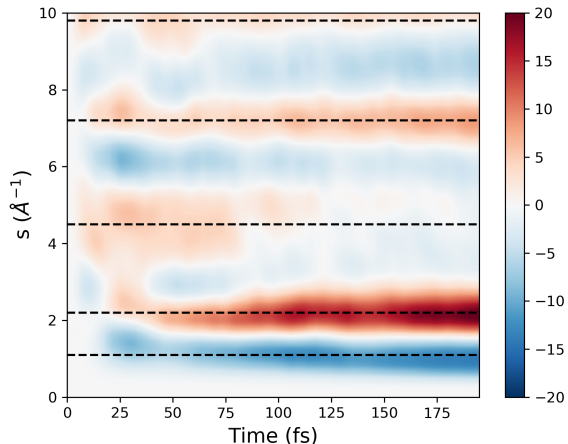


FIG. 3. Gas-phase UED pattern, $\%I_{\text{tot}}(s,t)$ in Eq. (13), for cyclobutanone calculated using the IAM with all trajectories and branches from our dynamics simulations. Five key features in the UED pattern are highlighted with horizontal dashed lines.

were taken from the trajectories showing each reaction observed and the IAM was then used to calculate the UED signal for each structure, briefly comprising of: a) α -CC bond breaking, b) β -CC bond breaking, c) the production of C_2H_4 , CH_2 and CO , and also d) production of CH_2CO and C_2H_4 . The structures for these pathways can be seen in the insets of Fig. 4.

Five key features can be observed in the gas-phase UED of cyclobutanone, these are highlighted by horizontal dashed lines in Fig. 3 at $s = 1.1, 2.2, 4.5, 7.2$ and 9.8 \AA^{-1} . Matching these peaks with those observed in Fig. 4, one can see all four reaction products yield a negative feature at $\sim 1.1 \text{ \AA}^{-1}$ and a positive feature at $\sim 2.2 \text{ \AA}^{-1}$. Both features at ~ 1.1 and $\sim 2.2 \text{ \AA}^{-1}$ grow in intensity after approximately 20 fs, matching the timescale shown in Section IV A. Both features continue to grow in intensity. Most notably, around 75 fs, Fig. 2 shows that we begin to observe α -CC bond breaking. This, coupled with the high intensity observed in the static signal of 4c) at 2.2 \AA^{-1} , suggest that the stepwise mechanism to form CO , C_2H_4 and CH_2 requires approximately 75 fs to form these products. However, we must note that the features in the signal have contributions from all the pathways shown in Fig. 4.

An additional broad positive feature can be observed centered at 4.5 \AA^{-1} , with a signal that decays after approximately 115 fs. Figure 4c) shows a broad negative feature between the values $\sim 3.75 \text{ \AA}^{-1}$ and $\sim 5.5 \text{ \AA}^{-1}$, indicating this reaction pathway causes the depletion of the broad signal. Once again due to the structural similarities of other reaction pathways, the net signal is a compounded signal with contributions from all products. A similar depletion can be seen in Fig. 4d), due to the higher proportion of trajectories being classified as belonging to d) this likely has a stronger effect on the signal.

Further peaks can be seen at 7.5 and 9.8 \AA^{-1} . A peak at 7.5 \AA^{-1} can be seen in all pathways with a similar intensity

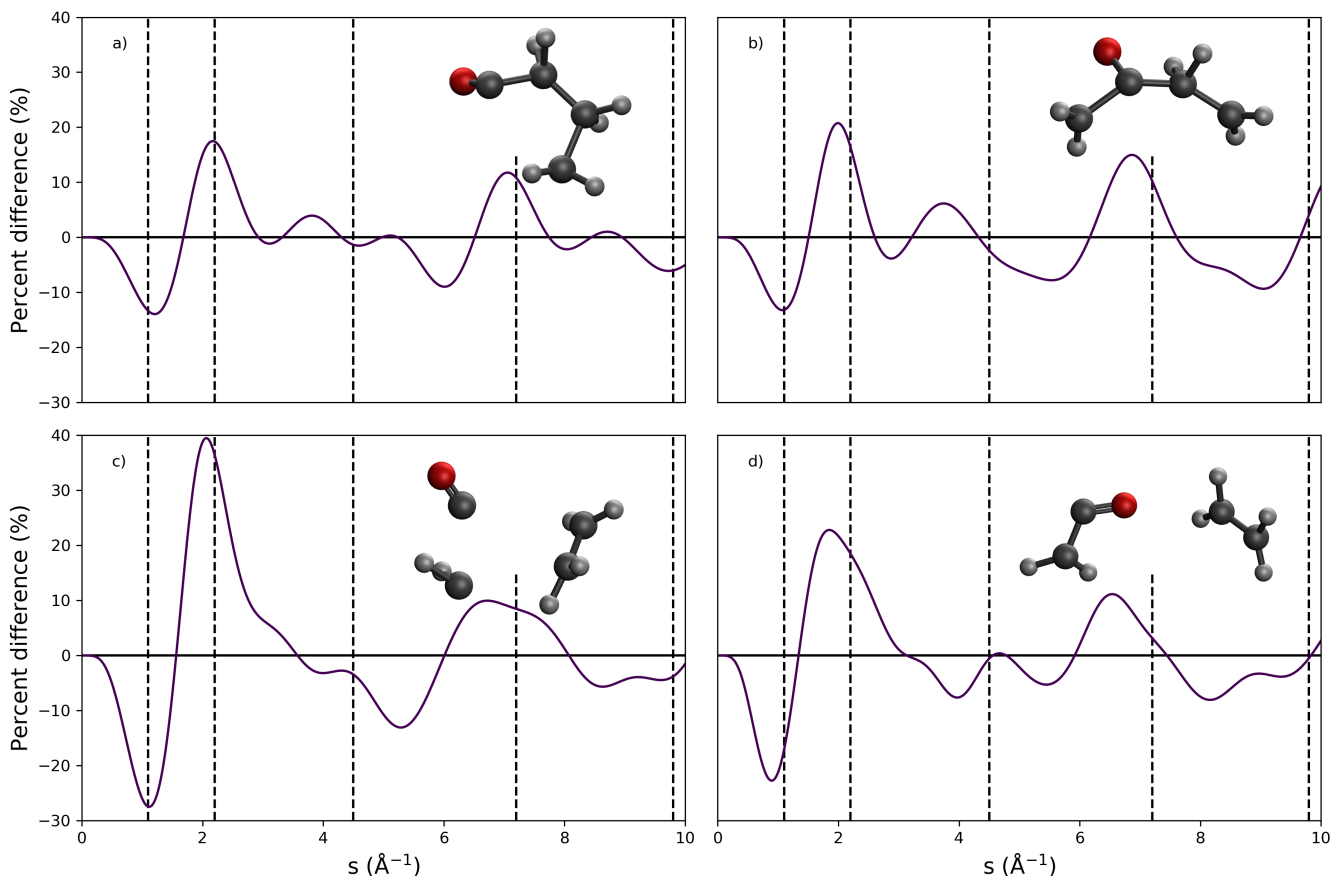


FIG. 4. Static signals obtained for representative structures of pathways observed in AIMC simulations given in percent differences. Panel a) α -CC ring opening, b) β -CC ring opening, c) dissociation to form CO, C₂H₄ and CH₂, and finally d) CH₂CO and C₂H₄. The structures shown as insets are the geometries from which the static signal is calculated. The five features shown in Figure 3 are highlighted with vertical dashed lines.

($\sim 10\%$) therefore yielding little structural information other than the molecule has moved away from the equilibrium geometry. In contrast, Fig. 4c) and to a lesser extent Fig. 4d) both show a signal at 9.8 \AA^{-1} . Thus, it is likely this feature arises from the breaking of the β -CC common to both reaction products.

V. CONCLUSIONS

This work was undertaken in response to the “*Prediction Challenge: Cyclobutanone Photochemistry*” and presents simulated ultrafast electron diffraction (UED) signals for gas-phase cyclobutanone upon photoexcitation into the S_2 electronic state. The main dissociation pathways of photoexcited cyclobutanone were identified with the help of AIMC non-adiabatic dynamics. Then, using these AIMC trajectories, the electronic diffraction was calculated using the IAM method. The calculated UED pattern was compared with static signals for representative structures for the different dissociation pathways observed in the AIMC dynamics. Overall, five key features in the UED pattern can be used to distinguish the reac-

tion channels observed in the AIMC simulation. We find that there is significant overlap between many features due to a high degree of structural similarity between the different photoproducts, combined with a significant degree of symmetry in cyclobutanone. However, ultimately, we found strong correlations between the timescales and products evident in the simulations and features in the overall UED signal (shown in Fig. 3).

The extent of the work was limited by the strict deadline inherent in the *Challenge*, and it is therefore straightforward to identify avenues for further work. To begin with, the presented simulations include only the first 200 fs of the cyclobutanone dissociation dynamics and the degree of sampling, i.e. the number of trajectories propagated, was also limited. Previously we developed a technique which allows to include the pump pulse shape into account and allows to account for the dynamics during the pulse³⁷. We have not used this approach here and assumed instant excitation, but it can be straightforwardly done. With longer propagation times it will also be easy to account for some coupling between coherent states, using the so called train basis functions²¹. This approach does not require additional trajectories and electronic structure cal-

culations. All of these improvements will be the subject of subsequent work. Longer simulation times will make it possible to make comparisons to the long-term dynamics observed in the experiment, while more trajectories should in principle allow us to move beyond the independent and semiclassical trajectory approximation used when calculating the UED signals. Also, as discussed in the UED theory section, should the experimental data indicate that more subtle effects in the scattering were observed, then *ab initio* simulations of the scattering signal, going beyond the independent atom model, are clearly of interest.

In summary, the present work demonstrates the capability of AIMC to simulate photodynamics in a challenging molecule and that UED signals can be predicted straightforwardly from the simulations. We also note that the AIMC simulations should in principle provide a better basis for the prediction of experimental signals that reflect the degree of coherence in the molecule during the dynamics, such as nonlinear spectroscopies or coherent mixed scattering.^{54,55}

ACKNOWLEDGEMENT

DM and DS acknowledge the support of EPSRC grant EP/P021123/1. AK acknowledges funding from the Leverhulme Trust (RPG-2020-208), and EPSRC grant EP/V049240.

- ¹D. Filippetto, P. Musumeci, R. Li, B. Siwick, M. Otto, M. Centurion, and J. Nunes, "Ultrafast electron diffraction: Visualizing dynamic states of matter," *Rev. Mod. Phys.* **94**, 045004 (2022).
- ²A. A. Ischenko, P. M. Weber, and R. J. D. Miller, "Capturing chemistry in action with electrons: Realization of atomically resolved reaction dynamics," *Chemical Reviews* **117**, 11066–11124 (2017).
- ³H. Yong, A. Kirrander, and P. M. Weber, "Time-resolved x-ray scattering of excited state structure and dynamics," in *Structural Dynamics with X-ray and Electron Scattering*, Theoretical and Computational Chemistry Series, Vol. 25, edited by K. Amini, A. Rouzée, and M. J. J. Vrakking (Royal Society of Chemistry, United Kingdom, 2024) 1st ed., Chap. 3, p. 344, www.rsc.org.
- ⁴B. Stankus, H. Yong, J. Ruddock, L. Ma, A. M. Carrascosa, N. Goff, S. Boutet, X. Xu, N. Zotev, A. Kirrander, M. Minitti, and P. M. Weber, "Advances in Ultrafast Gas-Phase X-ray Scattering," *J. Phys. B* **53**, 234004 (2020).
- ⁵J. Yang, V. Makhija, V. Kumarappan, and M. Centurion, "Reconstruction of three-dimensional molecular structure from diffraction of laser-aligned molecules," *Struct. Dyn.* **1**, 044101 (2014).
- ⁶T. Ishikawa, S. A. Hayes, S. Keskin, G. Corthey, M. Hada, K. Pichugin, A. Marx, J. Hirscht, K. Shionuma, K. Onda, Y. Okimoto, S.-y. Koshihara, T. Yamamoto, H. Cui, M. Nomura, Y. Oshima, M. Abdel-Jawad, R. Kato, and R. J. D. Miller, "Direct observation of collective modes coupled to molecular orbital-driven charge transfer," *Science* **350**, 1501–1505 (2015).
- ⁷M. Asenov, S. Ramamoorthy, N. Zotev, and A. Kirrander, "Inversion of Ultrafast X-ray Scattering with Dynamics Constraints," in *Machine Learning and the Physical Sciences* (2020) p. 7.
- ⁸H. Yong, A. M. Carrascosa, L. Ma, B. Stankus, M. P. Minitti, A. Kirrander, and P. M. Weber, "Determination of excited state molecular structures from time-resolved gas-phase X-ray scattering," *Faraday Disc.* **228**, 104–122 (2021).
- ⁹K. Acheson and A. Kirrander, "Robust Inversion of Time-Resolved Data via Forward-Optimization in a Trajectory Basis," *J. Chem. Theory Comp.* **19**, 2721–2734 (2023).
- ¹⁰C. R. Drury-Lessard and D. C. Moule, "Ring puckering in the $1B_2(n, 3s)$ Rydberg electronic state of cyclobutanone," *The Journal of Chemical Physics* **68**, 5392–5395 (1978).
- ¹¹L. O'Toole, P. Brint, C. Kosmidis, G. Boulakis, and P. Tsekeris, "Vacuum-ultraviolet absorption spectra of propanone, butanone and the cyclic ketones $C_nH_{2n-2}O$ ($n=4, 5, 6, 7$)," *J. Chem. Soc., Faraday Trans.* **87**, 3343–3351 (1991).
- ¹²R. F. Whitlock and A. B. Duncan, "Electronic spectrum of cyclobutanone," *The Journal of Chemical Physics* **55**, 218–224 (1971).
- ¹³T. S. Kuhlman, T. I. Sølling, and K. B. Møller, "Coherent Motion Reveals Non-Ergodic Nature of Internal Conversion between Excited States," *ChemPhysChem* **13**, 820–827 (2012).
- ¹⁴S. W. Benson and G. B. Kistiakowsky, "The Photochemical Decomposition of Cyclic Ketones," *Journal of the American Chemical Society* **64**, 80–86 (1942).
- ¹⁵H. O. Denschlag and E. K. C. Lee, "Benzene photosensitization and direct photolysis of cyclobutanone and cyclobutanone-2-t in the gas phase," *Journal of the American Chemical Society* **90**, 3628–3638 (1968).
- ¹⁶N. E. Lee and E. K. C. Lee, "Tracer Study of Photochemically Excited Cyclobutanone-2-t and Cyclobutanone. II. Detailed Mechanism, Energetics, Unimolecular Decomposition Rates, and Intermolecular Vibrational Energy Transfer," *The Journal of Chemical Physics* **50**, 2094–2107 (1969).
- ¹⁷E. K. C. Lee, R. G. Shorridge, and C. F. Rusbult, "Fluorescence excitation study of cyclobutanone, cyclopentanone, and cyclohexanone in the gas phase," *Journal of the American Chemical Society* **93**, 1863–1867 (1971).
- ¹⁸E. W. Diau, G. Köttig, and A. H. Zewail, "Femtochemistry of norrish type-1 reactions: ii. the anomalous predissociation dynamics of cyclobutanone on the S1 surface," *ChemPhysChem* **2**, 294–309 (2001).
- ¹⁹M. H. Kao, R. K. Venkatraman, M. N. Ashfold, and A. J. Orr-Ewing, "Effects of ring-strain on the ultrafast photochemistry of cyclic ketones," *Chemical Science* **11**, 1991–2000 (2020).
- ²⁰D. V. Makhov, W. J. Glover, T. J. Martinez, and D. V. Shalashilin, "Ab initio multiple cloning algorithm for quantum nonadiabatic molecular dynamics," *The Journal of Chemical Physics* **141**, 054110 (2014), https://pubs.aip.org/aip/jcp/article-pdf/doi/10.1063/1.4891530/13375170/054110_1_online.pdf.
- ²¹D. V. Makhov, C. Symonds, S. Fernandez-Alberti, and D. V. Shalashilin, "Ab initio quantum direct dynamics simulations of ultrafast photochemistry with multiconfigurational ehrenfest approach," *Chemical Physics* **493**, 200–218 (2017).
- ²²V. M. Freixas, S. Fernandez-Alberti, D. V. Makhov, S. Tretiak, and D. Shalashilin, "An ab initio multiple cloning approach for the simulation of photoinduced dynamics in conjugated molecules," *Phys. Chem. Chem. Phys.* **20**, 17762–17772 (2018).
- ²³D. V. Makhov, K. Saita, T. J. Martinez, and D. V. Shalashilin, "Ab initio multiple cloning simulations of pyrrole photodissociation: Tker spectra and velocity map imaging," *Phys. Chem. Chem. Phys.* **17**, 3316–3325 (2015).
- ²⁴J. A. Green, D. V. Makhov, N. C. Cole-Filipiak, C. Symonds, V. G. Stavros, and D. V. Shalashilin, "Ultrafast photodissociation dynamics of 2-ethylpyrrole: adding insight to experiment with ab initio multiple cloning," *Phys. Chem. Chem. Phys.* **21**, 3832–3841 (2019).
- ²⁵C. C. Symonds, D. V. Makhov, N. C. Cole-Filipiak, J. A. Green, V. G. Stavros, and D. V. Shalashilin, "Ultrafast photodissociation dynamics of pyrazole, imidazole and their deuterated derivatives using ab initio multiple cloning," *Phys. Chem. Chem. Phys.* **21**, 9987–9995 (2019).
- ²⁶D. V. Makhov and D. V. Shalashilin, "Simulation of the effect of vibrational pre-excitation on the dynamics of pyrrole photo-dissociation," *The Journal of Chemical Physics* **154**, 104119 (2021), https://pubs.aip.org/aip/jcp/article-pdf/doi/10.1063/5.0040178/13469571/104119_1_online.pdf.
- ²⁷D. V. Makhov, S. Adeyemi, M. Cowperthwaite, and D. V. Shalashilin, "Simulation of the dynamics of vibrationally mediated photodissociation for deuterated pyrrole," *Journal of Physics Communications* **6**, 025001 (2022).
- ²⁸D. V. Shalashilin, "Quantum mechanics with the basis set guided by Ehrenfest trajectories: Theory and application to spin-boson model," *The Journal of Chemical Physics* **130**, 244101 (2009), https://pubs.aip.org/aip/jcp/article-pdf/doi/10.1063/1.3153302/15995187/244101_1_online.pdf.
- ²⁹D. V. Shalashilin, "Nonadiabatic dynamics with the help of multiconfigurational Ehrenfest method: Improved theory and fully quantum 24D simulation of pyrazine," *The Journal of Chemical Physics* **132**, 244111 (2010), <https://pubs.aip.org/aip/jcp/article->

- pdf/doi/10.1063/1.3442747/16122321/244111_1_online.pdf.
- ³⁰D. V. Shalashilin, "Multiconfigurational Ehrenfest approach to quantum coherent dynamics in large molecular systems," *Faraday Discuss.* **153**, 105–116 (2011).
- ³¹K. Saita and D. V. Shalashilin, "On-the-fly ab initio molecular dynamics with multiconfigurational Ehrenfest method," *The Journal of Chemical Physics* **137**, 22A506 (2012), https://pubs.aip.org/aip/jcp/article-pdf/doi/10.1063/1.4734313/14003357/22a506_1_online.pdf.
- ³²B. F. E. Curchod and T. J. Martínez, "Ab Initio Nonadiabatic Quantum Molecular Dynamics," *Chemical Reviews* **118**, 3305–3336 (2018).
- ³³D. V. Shalashilin and M. S. Child, "Basis set sampling in the method of coupled coherent states: Coherent state swarms, trains, and pancakes," *The Journal of Chemical Physics* **128**, 054102 (2008), https://pubs.aip.org/aip/jcp/article-pdf/doi/10.1063/1.2828509/15411378/054102_1_online.pdf.
- ³⁴C. Symonds, J. A. Kattirtzi, and D. V. Shalashilin, "The effect of sampling techniques used in the multiconfigurational Ehrenfest method," *The Journal of Chemical Physics* **148**, 184113 (2018), https://pubs.aip.org/aip/jcp/article-pdf/doi/10.1063/1.5020567/15541045/184113_1_online.pdf.
- ³⁵V. M. Freixas, A. J. White, T. Nelson, H. Song, D. V. Makhov, D. Shalashilin, S. Fernandez-Alberti, and S. Tretiak, "Nonadiabatic excited-state molecular dynamics methodologies: Comparison and convergence," *The Journal of Physical Chemistry Letters* **12**, 2970–2982 (2021), pMID: 33730495, <https://doi.org/10.1021/acs.jpclett.1c00266>.
- ³⁶V. M. Freixas, W. Malone, X. Li, H. Song, H. Negrin-Yuvero, R. Pérez-Castillo, A. White, T. R. Gibson, D. V. Makhov, D. V. Shalashilin, Y. Zhang, N. Fedik, M. Kulichenko, R. Messerly, L. N. Mohanam, S. Sharifzadeh, A. Bastida, S. Mukamel, S. Fernandez-Alberti, and S. Tretiak, "Nexmd v2.0 software package for nonadiabatic excited state molecular dynamics simulations," *Journal of Chemical Theory and Computation* **19**, 5356–5368 (2023), pMID: 37506288, <https://doi.org/10.1021/acs.jctc.3c00583>.
- ³⁷D. V. Makhov and D. V. Shalashilin, "Floquet hamiltonian for incorporating electronic excitation by a laser pulse into simulations of non-adiabatic dynamics," *Chemical Physics* **515**, 46–51 (2018), ultrafast Photoinduced Processes in Polyatomic Molecules: Electronic Structure, Dynamics and Spectroscopy (Dedicated to Wolfgang Domcke on the occasion of his 70th birthday).
- ³⁸A. Moreno Carrascosa, H. Yong, D. L. Crittenden, P. M. Weber, and A. Kirrander, "Ab Initio Calculation of Total X-ray Scattering from Molecules," *J. Chem. Theory Comput.* **15**, 2836–2846 (2019).
- ³⁹R. M. Parrish and T. J. Martínez, "Ab initio computation of rotationally-averaged pump-probe x-ray and electron diffraction signals," *J. Chem. Theory Comp.* **0**, null (2019), pMID: 30702882, <https://doi.org/10.1021/acs.jctc.8b01051>.
- ⁴⁰N. Zotev, A. Moreno Carrascosa, M. Simmermacher, and A. Kirrander, "Excited Electronic States in Total Isotropic Scattering from Molecules," *J. Chem. Theory Comput.* **16**, 2594–2605 (2020).
- ⁴¹A. M. Carrascosa, J. P. Coe, M. Simmermacher, M. J. Paterson, and A. Kirrander, "Towards high-resolution X-ray scattering as a probe of electron correlation," *Phys. Chem. Chem. Phys.* **24**, 24542–24552 (2022).
- ⁴²A. Kirrander, K. Saita, and D. V. Shalashilin, "Ultrafast X-ray Scattering from Molecules," *J. Chem. Theory Comput.* **12**, 957–967 (2016).
- ⁴³M. Stefanou, K. Saita, D. V. Shalashilin, and A. Kirrander, "Comparison of ultrafast electron and x-ray diffraction – a computational study," *Chem. Phys. Lett.* **683**, 300–305 (2017).
- ⁴⁴A. Kirrander and P. M. Weber, "Fundamental Limits on Spatial Resolution in Ultrafast X-ray Diffraction," *Appl. Sci.* **7**, 534 (2017).
- ⁴⁵N. F. Mott and W. L. Bragg, "The scattering of electrons by atoms," *Proc. R. Soc., Lond., Ser. A* **127**, 658–665 (1930).
- ⁴⁶H. Bethe, "Zur Theorie des Durchgangs schneller Korpuskularstrahlen durch Materie," *Ann. Phys.* **397**, 325–400 (1930).
- ⁴⁷M. Simmermacher, P. M. Weber, and A. Kirrander, "Theory of time-dependent scattering," in *Structural Dynamics with X-ray and Electron Scattering*, Theoretical and Computational Chemistry Series, Vol. 25, edited by K. Amini, A. Rouzée, and M. J. J. Vrakking (Royal Society of Chemistry, United Kingdom, 23 December 2023) 1st ed., Chap. 3, p. 85, www.rsc.org.
- ⁴⁸E. Prince, ed., *International Tables for Crystallography Volume C: Mathematical, physical and chemical tables*, 2006th ed., ISBN 978-1-4020-1900-5 (Wiley, 2006).
- ⁴⁹F. Salvat, "Elastic scattering of fast electrons and positrons by atoms," *Phys. Rev. A* **43**, 578–581 (1991).
- ⁵⁰F. Salvat, A. Jablonski, and C. J. Powell, "elsepa—Dirac partial-wave calculation of elastic scattering of electrons and positrons by atoms, positive ions and molecules," *Comput. Phys. Commun.* **165**, 157–190 (2005).
- ⁵¹P. Debye, "Zerstreuung von Röntgenstrahlen," *Ann. Phys.* **351**, 809–823 (1915).
- ⁵²H.-J. Werner, P. J. Knowles, F. R. Manby, J. A. Black, K. Doll, A. Heßelmann, D. Kats, A. Köhn, T. Korona, D. A. Kreplin, Q. Ma, I. Müller, Thomas F., A. Mitrushchenkov, K. A. Peterson, I. Polyak, G. Rauhut, and M. Sibaev, "The Molpro quantum chemistry package," *The Journal of Chemical Physics* **152**, 144107 (2020), https://pubs.aip.org/aip/jcp/article-pdf/doi/10.1063/5.0005081/16680626/144107_1_online.pdf.
- ⁵³T. S. Kuhlman, S. P. A. Sauer, T. I. Sølling, and K. B. Møller, "Symmetry, vibrational energy redistribution and vibronic coupling: The internal conversion processes of cycloketones," *The Journal of Chemical Physics* **137** (2012), 10.1063/1.4742313.
- ⁵⁴M. Simmermacher, A. Moreno Carrascosa, N. E. Henriksen, K. B. Møller, and A. Kirrander, "Theory of ultrafast x-ray scattering by molecules in the gas phase," *J. Chem. Phys.* **151**, 174302 (2019).
- ⁵⁵D. Keefer, F. Aleotti, J. R. Rouxel, F. Segatta, B. Gu, A. Nenov, M. Garavelli, and S. Mukamel, "Imaging conical intersection dynamics during azobenzene photoisomerization by ultrafast x-ray diffraction," *Proc. Natl. Acad. Sci. U.S.A.* **118** (2021), <https://www.pnas.org/content/118/3/e2022037118.full.pdf>.